Aspirin-triggered resolvin D1 reduces parasitic cardiac load by decreasing inflammation through N-formyl peptide receptor 2 in a chronic murine model of Chagas disease

Short title: Aspirin-triggered resolvin D1 in Chagas disease

Ileana Carrillo[1], Rayane Rabelo[2,3], César Barbosa[2], Mariana Rates[2], Sebastián Fuentes-Retamal[1], Fabiola González-Herrera[1], Daniela Guzmán-Rivera[1,4], Helena Quintero[1], Ulrike Kemmerling[5], Christian Castillo[6], Fabiana S. Machado[2,3], Guillermo Díaz-Araya[7*], Juan D. Maya[1*]

[1]Programa de Farmacología Molecular y Clínica, ICBM, Facultad de Medicina, Universidad de Chile, Santiago, Chile

[2] Laboratório de Imunorregulação de Doenças Infecciosas, Departamento de Bioquímica e Imunologia, ICB, Universidade Federal de Minas Gerais, Belo Horizonte, Brazil

[3] Programa em Ciências da Saúde, Doenças Infecciosas e Medicina Tropical/ Laboratório Interdisciplinar de Investigação Médica, Faculdade de Medicina, Universidade Federal de Minas Gerais, Belo Horizonte, MG, Brazil

[4] Escuela de Farmacia, Facultad de Medicina, Universidad Andrés Bello, Santiago, Chile

[5]Programa de Anatomía y Biología del Desarrollo, ICBM, Facultad de Medicina, Universidad de Chile, Santiago, Chile

[6]Facultad de Medicina Veterinaria y Agronomía, Universidad de Las Américas, Santiago, Chile

[7] Departamento de Farmacología Química y Toxicología, Facultad de Ciencias Químicas y Farmacéuticas, Universidad de Chile, Santiago, Chile

*Corresponding authors

E-mail: jdmaya@uchile.cl (JDM); gadiaz@ciq.uchile.cl (GD)

ABSTRACT

Chagas disease, caused by the protozoan *Trypanosoma cruzi*, is endemic in Latin America and is widely distributed worldwide because of migration. After years of infection and in the absence of treatment, the disease progresses from an acute and asymptomatic phase to a chronic inflammatory cardiomyopathy, leading to heart failure and death. An inadequate balance in the inflammatory response is involved in the progression of chronic Chagas cardiomyopathy. Current therapeutic strategies cannot prevent or reverse the heart damage caused by the parasite. Aspirin-triggered resolvin D1 (AT-RvD1) is a pro-resolving mediator of inflammation that acts through N-formyl peptide receptor 2 (FPR2). AT-RvD1 participates in the modification of cytokine production, inhibition of leukocyte recruitment and efferocytosis, macrophage switching to a nonphlogistic phenotype, and the promotion of healing, thus restoring organ function. In the present study, AT-RvD1 is proposed as a potential therapy aid to regulate the pro-inflammatory state during the chronic phase of Chagas disease. C57BL/6 wild-type and FPR2 knock-out mice chronically infected with *T. cruzi* were treated for 20 days with 5 μg/kg/day AT-RvD1, 30 mg/kg/day benznidazole, or the combination of 5 μg/kg/day AT-RvD1 and 5 mg/kg/day benznidazole. At the end of treatment, changes in the immune response, cardiac tissue damage, and parasite load were evaluated. The administration of AT-RvD1 in the chronic phase of *T. cruzi* infection regulated the inflammatory response both at the systemic level and in the cardiac tissue, and it reduced cellular infiltrates, cardiomyocyte hypertrophy, fibrosis, and the parasite load in the heart tissue. Thus, AT-RvD1 was shown to be an attractive therapeutic due to its regulatory effect on the inflammatory response at the cardiac level and its ability to reduce the parasite load during chronic *T. cruzi* infection, thereby preventing the chronic cardiac damage induced by the parasite.

Author Summary:

Chagas disease is prevalent in Latin America and is widely distributed worldwide due to migration. If the parasite is left untreated, the disease progresses from an acute symptomless phase to chronic myocardial inflammation, which can cause heart failure and death years after infection. Imbalances in the inflammatory response are related to this progression. Current treatments cannot prevent or reverse the cardiac damage produced by the parasite. Aspirin-triggered resolvin D1, also named AT-RvD1, can modify cellular and humoral inflammatory responses leading to the resolution of inflammation, thus promoting healing and restoring organ function. In this study, AT-RvD1, in an N-formyl peptide receptor 2 (FPR2)-dependent manner, was shown to regulate local and systemic inflammation and decrease cellular infiltration in the heart tissue of mice chronically infected with the parasite and reduce cardiac hypertrophy and fibrosis. Importantly, AT-RvD1 was able to decrease parasite load in the infected hearts. Thus, this research indicates that At-RvD1 treatment is a potential therapeutic strategy that offers an improvement on current drug therapies.

Keywords: Chagas disease, cardiomyopathy, AT-RvD1, inflammation, immunomodulation, immunoregulation

Introduction

Chagas disease (CD) is caused by the protozoan *Trypanosoma cruzi*, which afflicts 7 million people in 21 endemic Latin American countries and is increasing in non-endemic countries due to migration (WHO, 2018). According to the World Health Organization [1], the most alarming statistics are that 30000 new cases, of which 8000 are newborns, are reported annually and there are more than 10000 deaths per year. Only 1% of patients receive adequate and opportune treatment. Clinically, CD initially presents an acute phase, generally asymptomatic, but in the absence of treatment a chronic phase develops. In 30% of chronic cases, patients develop cardiac or digestive complications 10-30 years after acquiring the infection [2, 3]. Chronic Chagas cardiomyopathy (CCC) is considered the most frequent and severe clinical manifestation of CD. It is characterized by focal inflammatory infiltrates, cardiac hypertrophy, and fibrosis, leading to abnormalities in the electrical conduction system and heart failure [4]. Sudden death is the leading cause of mortality in patients with CCC [5]. Chronic inflammation is considered one of the most important mechanisms involved in the pathogenesis of CD and has been proposed as a consequence of tissue damage due to the persistence of live parasites [6]. This chronic inflammation is a determining factor in the deterioration of heart architecture and loss of functionality [7]. The current treatment for CD utilizes nitroheterocyclic drugs, such as benznidazole (Bz), which are far from efficacious. For that reason, new approaches for treating this disease or improving the action of current antiparasitic drugs are needed.

Acute inflammation is a natural protective mechanism of the host in response to injury or invading pathogens. The resolution of inflammation is an active process orchestrated by molecules known as specialized pro-resolving mediators (SPM) that culminate inflammatory processes [8]. Endogenous SPMs actively participate in the dampening of host responses and the resolution of inflammation. Mainly produced by macrophages and neutrophils from distinct omega-3 polyunsaturated fatty acid pathways, the four families of SPMs, lipoxins, maresins, protectins, and resolvins, have been shown

105 to act as initiators of the resolution of acute inflammation; therefore, they limit polymorphonuclear
106 neutrophil infiltration, counteract the production of cytokines and chemokines, and enhance
107 macrophage-mediated actions [9]. Resolvin D1 (RvD1) is a novel SPM whose effects on
108 inflammatory diseases dampen pathological inflammatory responses and restore tissue homeostasis
109 [10]. Some drugs such as acetylsalicylic acid (ASA) modify the activity of cyclooxygenase 2
110 (COX-2), allowing SPM epimer generation, specifically 15-epi-LXA_4 and AT-RvD1-4 [11, 12].
111 These "aspirin-triggered" SPMs have the advantage of being more stable to enzymatic degradation
112 than endogenous molecules and can serve as anti-inflammatory drugs [11, 13].

113 In CD, ASA has been extensively studied and beneficial effects have been reported closely related
114 to its dose. In experimental models, a low dose of ASA (25 mg/kg) improves survival, reduces heart
115 inflammatory infiltrates, and improves cardiac tissue architecture. These effects were associated
116 with a significant increase in the production of 15-epi-LXA_4 [14]. Moreover, this aspirin-triggered
117 lipoxin reduces the internalization of *T. cruzi* in macrophages [15], an effect mediated by N-formyl
118 peptide receptor 2 (FPR2) [16, 17]. These effects have highlighted the role of FPR2 in the beneficial
119 effects of ASA. In recent years, the effects of AT-RvD1 on CD have been reported in several
120 publications. First, on peripheral mononuclear cells (PBMCs) from patients with stage B1 Chagas
121 heart disease (having few cardiac abnormalities), AT-RvD1 had an immunomodulatory effect by
122 decreasing the production of pro-inflammatory cytokines such as interferon-gamma (IFNγ) and the
123 proliferation of PBMCs after stimulation with *T. cruzi* antigen, counteracting the inflammatory
124 environment [18]. Second, the effect of RvD1 was recently studied in a murine model chronically
125 infected with *T. cruzi*, where RvD1 therapy increased the survival rate and regulated the
126 inflammatory response by reducing serum IFNγ levels and increasing serum IL-10 levels.
127 Furthermore, RvD1 reduced inflammatory infiltrates, favoring the resolution of *T. cruzi* infection
128 and preventing cardiac fibrosis [19].

After infection in mammals, *T. cruzi* induces robust innate and adaptive immune responses, which play a significant role during the acute and chronic phases of the disease. Nonetheless, these responses are insufficient to achieve complete clearance of the parasite, and parasite persistence promotes low and sustained inflammation over time [6]. Therefore, because of the benefits of AT-RvD1 in reducing pathological inflammatory processes and promoting restoration of tissue homeostasis, it is possible that AT-RvD1 administration in CD aids in the prevention of inflammatory damage secondary to parasite persistence and in parasite clearance. In the present study, we evaluated the effects of AT-RvD1 and whether Bz and AT-RvD1 combined therapy could improve parasite control and reduce inflammation, heart damage, and irregular cardiac electrical activity, limiting the progress of CCC in a murine model of chronic CD. Thus, we have identified AT-RvD1 as a new potential therapeutic approach to modulate the pathogenesis of CD.

151 **Methods**

152 Animals

153 Animal care and handling procedures were in accordance with the guidelines of the local animal
154 ethics committee. Eight to ten-week-old C57BL/6 wild-type (WT) mice were obtained from the
155 Animal Care Facilities of Universidade Federal de Minas Gerais (UFMG, Brazil). The FPR2
156 knockout mice were bred on a C57BL/6 genetic background under pathogen-free conditions at the
157 Instituto de Ciências Biológicas – UFMG. The animals were randomly distributed and were housed
158 at 2 to 3 animals per box in a controlled environment at constant temperature, under a 12-h
159 day/night cycle, and with food and water available *ad libitum*. This research study was carried out
160 in strict accordance with the Brazilian Guidelines on animal work and the Guide for the Care and
161 Use of Laboratory Animals of the National Institutes of Health (NIH). The Institutional Bioethics
162 Committee of the Faculty of Medicine, University of Chile, approved the supervising protocols
163 (Protocol CBA# 1078 FMUCH, associated with FONDECYT-Chile grant number 1170126).

164 Parasites and infection protocols

165 Dm28c trypomastigotes from Vero cell cultures (1×10^5) were used to intraperitoneally inoculate
166 the C57Bl/6 mice. At the peak of parasitemia, blood was collected and pooled from various donors,
167 and the parasites were counted by direct visualization of a drop of blood under a light microscope.
168 Finally, the trypomastigotes were suspended in sterile saline, and 1×10^3 trypomastigotes in 100 µL
169 were injected into each experimental animal. After randomization, the animals were divided into
170 five groups (healthy groups) or eight groups (infections and different treatments). *T. cruzi* infection
171 was confirmed from the third day after infection by direct microscopic visualization of circulating
172 trypomastigotes in peripheral blood samples obtained from the tail tip. Subsequently, the
173 parasitemia was monitored every two days via peripheral blood samples until undetectable [14].

174 Treatment protocols

175 Infected C57BL/6 WT and FPR2$^{-/-}$ mice were treated with 5 µg/kg/day aspirin-triggered Resolvin
176 D1 (AT-RvD1) (Cayman Chemicals®, Ann Harbor, MI, USA), 30 mg/kg/day Bz (Abarax - Elea
177 Laboratory, Buenos Aires, Argentina), or a combination of 5 µg/kg/day AT-RvD1 + 5 mg/kg/day
178 Bz. The Bz was suspended in 0.5% carboxymethylcellulose and administered orally once a day.
179 AT-Rv1 was dissolved in 0.01% ethanol and administered intraperitoneally once a day. The
180 treatments were administered from day 40 to 60 post-infection (p.i.). On day 60 p.i., the animals
181 were anesthetized with 100 mg/kg ketamine and 10 mg/kg xylazine, and their blood and hearts
182 removed. The hearts were halved, with one half fixed in 4% formaldehyde in 0.1 M phosphate-
183 buffered saline (PBS; pH 7.3) for histological analysis and the other half extracted in TRIzol™
184 (Invitrogen, Waltham, MA, USA) for mRNA expression analysis by RT-qPCR.

185 Enzyme-linked immunosorbent assay (ELISA)

186 Peripheral blood was collected from the submandibular vein of the C57BL/6 mice on days 20 and
187 40 p.i. On day 60, whole blood was collected after euthanasia. The blood was centrifuged, and the
188 resulting serum was stored at -80 °C. Cytokine quantification was performed on the serum samples
189 by ELISA using specific mouse monoclonal antibodies from the ELISA Max Deluxe Set for mouse
190 tumor necrosis factor alpha (TNFα), IFNγ, interleukin (IL)-1β, and IL-10 (BioLegend, San Diego,
191 CA, USA), following the manufacturer's instructions. The absorbance of the ELISA plate wells was
192 read at 450 nm in a microplate reader Biotek® (Winooski, VT, USA). All samples were analyzed in
193 duplicate.

194 Quantitative reverse transcription PCR (RT-qPCR) assay

195 For measurements of cytokine gene expression in cardiac tissue, total RNA was isolated using
196 TRIzol™ reagent, followed by DNAse treatment and purification using the PureLink RNA Mini Kit
197 (Thermo Fisher Waltham, MA, USA) according to the manufacturer's instructions. cDNA was
198 synthesized from 600 ng of total RNA by reverse transcription using M-MLV reverse transcriptase

199 and random primers (Invitrogen). For the qPCR analyses, each reaction mix contained 150 nM of
200 each primer (forward and reverse), 1 ng of sample cDNA, 7 μL of SensiMix™ SYBR® Green
201 Master Mix (Bioline®, Memphis, TE, USA), and H_20 in a total volume of 15 μL. The primers used
202 for the analysis of cytokines and hypertrophy markers were the following: TNFα, Fw: 5′-
203 TAGCCCACGTCGTAGCAAAC-3′ and Rv: 5′-ACAAGGTACAACCCATCGGC-3′; IFNγ, Fw:
204 5′-AACTGGCAAAAGGATGGTGAC-3′ and Rv: 5′-TTGCTGATGGCCTGATTGTC-3′; IL-1β,
205 Fw: 5′-TGCCACCTTTTGACAGTGATG-3′ and Rv: 5′-GTGCTGCTGCGAGATTTGAA-3′; IL-
206 10, Fw: 5′-ACCTGGTAGAAGTGATGCCC-3′ and Rv: 5′-ACAGGGGAGAAATCGATGACAG-
207 3′; atrial natriuretic peptide (ANP), Fw: 5′-GGGCTTCTTCCTCGTCTTGG-3′ and Rv: 5′-
208 GTGGTCTAGCAGGTTCTTGAAAT-3′; brain natriuretic peptide (BNP), Fw: 5′-
209 CAGAGCAATTCAAGATGCAGAAGC-3′ and Rv: 5′-CTGCCTTGAGACCGAAGGAC-3′. The
210 amplification was performed in an ABI Prism 7300 sequence detector (Applied Biosystems®,
211 Waltham, MA, USA). The cycling program was as follows: a denaturation step at 95 °C for 3 min
212 and 40 amplification cycles of 95 °C (15 s), 60 °C (15 s), and 72 °C (30 s). The final step was a
213 dissociation stage that ramped from 60 to 95 °C over 100 s. For relative quantification, the results
214 were expressed as RQ values determined using the comparative control (delta-delta-Ct (DDCt))
215 method [20].

216 The presence of viable parasites in cardiac tissue was evaluated by amplification of 18S *T. cruzi*
217 ribosomal RNA (rRNA). For this purpose, total RNA was isolated using TRIzol™ and purified
218 using the PureLink RNA Mini Kit; cDNA was synthesized as detailed above. RT-qPCR was
219 performed as described above with the following primers: 18S, Fw: 5′-
220 TGGAGATTATGGGGCAGT-3′ and Rv: 5′-GTTCGTCTTGGTGCGGTCTA-3′. The parasitic
221 load of *T. cruzi* in the cardiac tissues was calculated from a standard curve constructed using 1 ×
222 10^8 trypomastigotes of *T. cruzi*, serially diluted to provide a log curve in the range of 1 to 10^8
223 equivalent parasites/10 ng of tissue RNA.

224 Histology

225 The hearts from the euthanized mice were fixed in 4% formaldehyde (pH 7.3). Then, the fixed heart
226 tissues were dehydrated with 50 to 100% ethanol, clarified with xylol, embedded in paraffin, and
227 sectioned in 5 μm slices. The sections were stained with hematoxylin and eosin to observe cellular
228 infiltration and cardiomyocyte cross-sectional area or with picrosirius red to observe collagen
229 organization. Images were obtained using a spinning-disk microscope (Olympus BX42). Five fields
230 per heart (40X) were analyzed using Image J software.

231 For the analysis of cellular infiltrates, the nuclei present in five fields of each heart were quantified.
232 The number of nuclei per tissue area was counted in order to eliminate empty tissue areas. In the
233 analysis of cardiomyocyte cross-sectional area, only muscle fibers with well-defined borders and a
234 nucleus inside were included. For the analysis of fibrosis in the picrosirius red-stained slides, the
235 red-colored pixels in the cardiac tissue were quantified in five fields per animal.

236 Electrocardiogram (ECG) recording and analysis

237 ECG recording was performed using a six-channel non-invasive electrocardiograph (ECG-PC
238 version 2.07, Electronic Technology of Brazil (TEB), Belo Horizonte/MG, Brazil). The mice were
239 anesthetized initially with 2.5% isoflurane and then maintained with 1.5% isoflurane (VetCase-
240 Incotec, Serra/ES, Brazil). The mice were placed in a dorsal recumbent position on a wooden table
241 covered with plastic material; electrocardiographic gel was applied, and four alligator clip
242 electrodes were attached to the skin of the forelimbs and hindlimbs. All procedures were performed
243 in a quiet room to minimize stress.

244 All ECGs were performed and analyzed by the same technician according to standard methods for
245 ECG trace analysis. The tracings were recorded from six leads of the frontal plane at a velocity of
246 50 mm/s. In each tracing, three segments containing five beats (lead II) were selected for quality
247 (clean baseline with no artifacts), and the mean values for heart rate (HR) and duration of the

intervals and waves were determined. The parameters evaluated were heart rate, P wave, QRS complex, PR interval, and QT interval. QT-corrected values were obtained from Bazett's formula.

Statistical analysis

For all experiments, statistical significance was established at p values of 0.05. The data represent the means ± standard deviations (SD) from at least three independent observations or experiments. All statistical analyses were performed using GraphPad Prism 8.0 software. One-way and two-way analyses of variance (ANOVAs) (with Tukey's post-hoc tests) were performed as appropriate. A log-rank test was performed for survival analysis.

Results

Effect of the absence of FPR2 on *T. cruzi* parasitemia

The progression of parasitemia and mortality in C57BL/6 WT and FPR2$^{-/-}$ mice infected with *T. cruzi* strain Dm28c were determined to evaluate the establishment of a murine model for chronic CD (Fig 1). As expected, in the WT mice, detectable parasitemia persisted for approximately 40 days, with the peak of infection occurring at 27 days p.i. (Fig 1A). In the FPR2$^{-/-}$ mice, the parasitemia level was significantly lower in the second peak of infection, but the overall kinetics during the acute phase was similar to that of the WT mice.

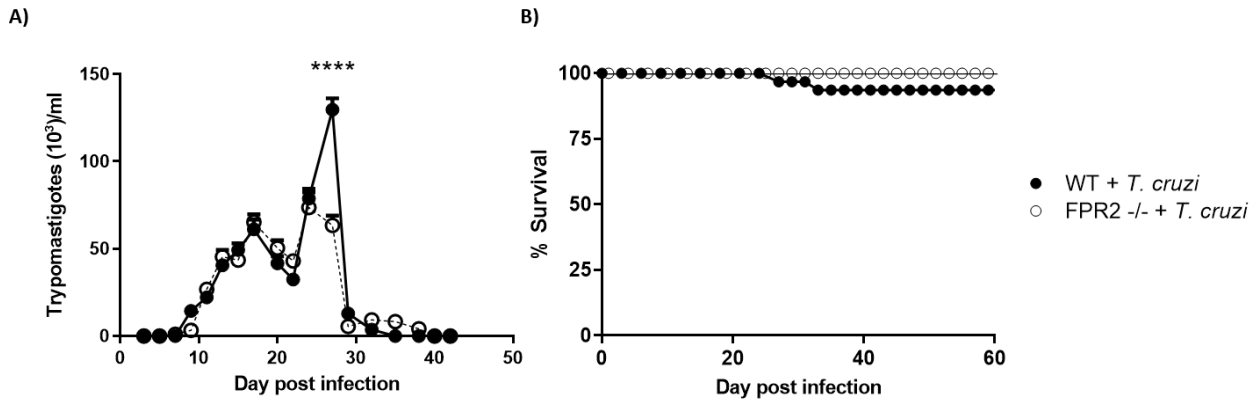

Fig 1. Parasitemia and survival in C57BL/6 wild-type (WT) or FPR2 knock-out (FPR2 -/-) mice infected with *Trypanosoma cruzi* (Dm28c). A) Blood parasite levels, B) Kaplan-Meier survival curves. Data are expressed as the mean ± SD (n = 8). Two-way ANOVA was performed to identify significant differences, ****$p \leq 0.0001$.

Furthermore, survival rates were high for all mice until the end of the experiment, regardless of their genetic background, confirming that the mortality of this murine model of *T. cruzi* chronic infection was low.

Regarding inflammatory responses, changes in serum levels of pro-inflammatory (TNFα, IFNγ, IL-1β) and anti-inflammatory cytokines (IL-10) were determined at days 20, 40, and 60 p.i. in WT and FPR2$^{-/-}$ mice infected with *T. cruzi* (S1 A, C, E, and G Fig). Both the healthy WT and FRP2$^{-/-}$ mice showed differences in serum cytokine levels at baseline and after *T. cruzi* infection. The healthy FPR2$^{-/-}$ mice had elevated levels of TNFα and IL-10 compared to those of the healthy WTs (S1 A and G Fig). In addition, the magnitude of the inflammatory response was higher in the WT mice than in the FPR2$^{-/-}$ mice (S1B, D, and H Fig). At day 40 p.i., the infected WT mice still maintained slightly increased TNFα, IFNγ, and IL-10 levels compared to their healthy controls, while the FPR2$^{-/-}$ mice only had slightly increased IFNγ levels. These findings indicate that the FPR2$^{-/-}$ mice developed a different immune response against *T. cruzi* infection than the WT mice (S1 Fig).

285 Effect of AT-RvD1 treatment on the inflammatory state in CD

286 The effect of AT-RvD1 treatment on inflammation in chronic CD was evaluated by measuring
287 serum cytokine levels at the end of treatment (60 dpi). Consistent with a chronic inflammatory state,
288 the serum levels of pro-inflammatory cytokines such as TNFα (Fig 2A), IFNγ (Fig 2B), and IL-1β
289 (Fig 2C) increased as a result of the infection in the WT and FPR2$^{-/-}$ mice, although the IL-1β
290 increase in the FPR2$^{-/-}$ mice was not significant. Unexpectedly, AT-RvD1 did not reduce serum
291 TNFα levels in the WT mice (Fig 2A); however, AT-RvD1 treatment significantly reduced the
292 serum levels of IFNγ (Fig 2B) and IL-1β (Fig 2C), reaching healthy control levels. This effect was
293 mediated by FPR2 because in the FPR2$^{-/-}$ mice, AT-RvD1 treatment did not alter IFNγ levels. In
294 contrast, Bz, alone or combined with AT-RvD1, did not affect the increased serum levels of pro-
295 inflammatory cytokines, except for IL-1β in the WT mice (Fig 2C). Either treatment produced
296 negligible effects on Il-10 (Fig 2D).

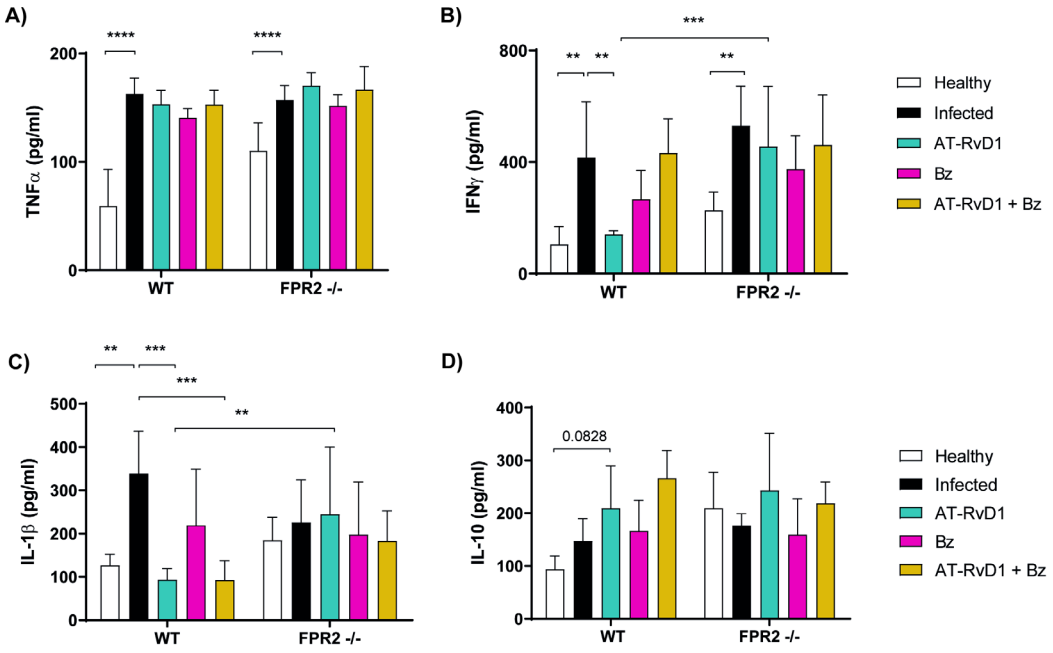

297

298 **Fig 2. Serum cytokine levels in mice infected with *Trypanosoma cruzi* and treated with AT-**
299 **RvD1 and/or Bz at 60 days post-infection.** The concentrations of TNFα (A), IFNγ (B), IL-1β (C),

300 and IL-10 (D) in serum were quantified by ELISA. Data are expressed as the mean ± SD (*n* = 5).
301 Two-way ANOVAs and Tukey's post-hoc tests were performed to identify significant differences.
302 **$p \leq 0.01$, ***$p \leq 0.001$, ****$p \leq 0.0001$. Bz, benznidazole; AT-RvD1, aspirin-triggered resolvin
303 D1.

304 Because serum cytokine levels reflect systemic inflammatory states, it was also necessary to
305 measure them in the heart to determine local inflammatory states. Thus, the effect on the immune
306 response in cardiac tissue was determined by measuring relative cytokine mRNA levels after 20
307 days of treatment with AT-RvD1 (60 dpi). In this case, mRNA levels of the pro-inflammatory
308 TNFα (Fig 3A), IFNγ and IL-1β (Fig 3C) cytokines were increased in both the WT and $FPR2^{-/-}$
309 infected mice. Although the mRNA levels of IFNγ were exceedingly increased with the infection, it
310 was not modified by At-RvD1 or Bz in WT and $FPR2^{-/-}$ mice (Fig 3B). Interestingly, in the WT and
311 $FPR2^{-/-}$ mice, AT-RvD1 treatment significantly increased IL-10 expression levels (Fig 3D). AT-
312 RvD1 prevented the increase in TNFα caused by infection. Neither Bz nor combinatorial therapy
313 modified the mRNA levels of the measured cytokines.

314

315

316

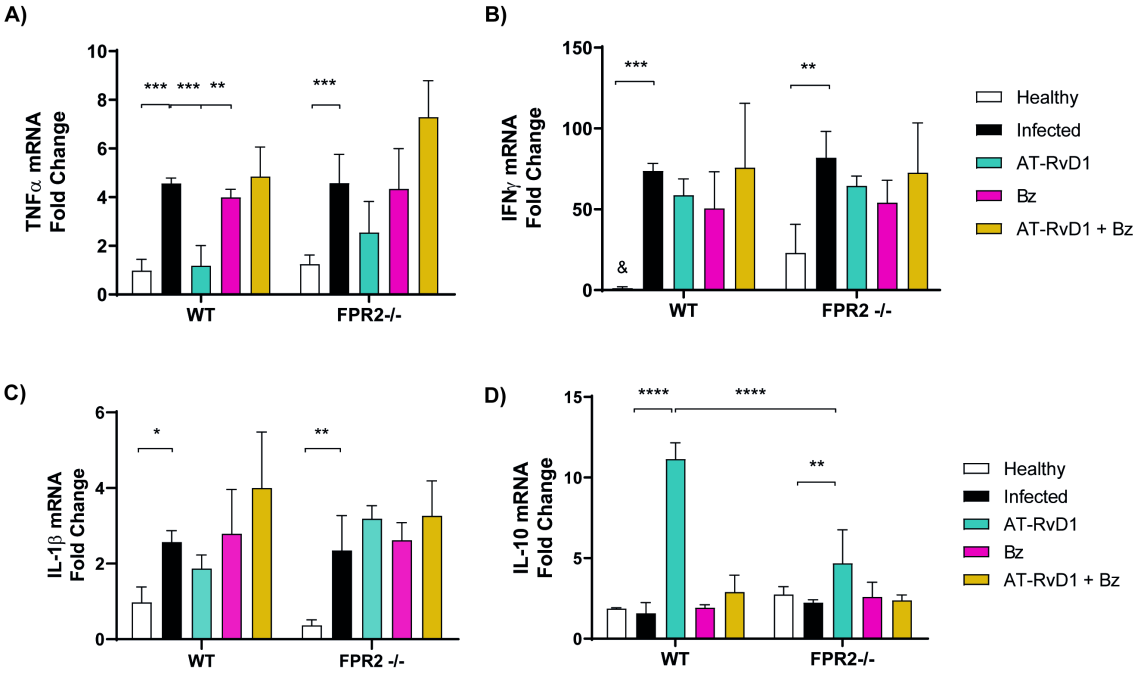

Fig 3. Cytokine mRNA levels in cardiac tissue of mice infected with *Trypanosoma cruzi* and treated with AT-RvD1 or Bz at 60 days post-infection. The cardiac mRNA levels of TNFα (A), IFNγ (B), IL-1β (C), and IL-10 (D) are shown from uninfected C57BL/6 mice infected with *T. cruzi* and treated with AT-RvD1 and Bz, as assessed by RT-qPCR. Data are expressed as the mean ± SD (n = 5). Two-way ANOVAs and Tukey's post-hoc tests were performed to identify significant differences. *$p \leq 0.05$, **$p \leq 0.01$, ***$p \leq 0.001$, ****$p \leq 0.0001$. & indicates indeterminate values. Bz, benznidazole; AT-RvD1, aspirin-triggered resolvin D1.

In CCC, chronic inflammation is a determining factor in the deterioration of heart architecture. The cellular infiltrates in heart tissue sections were measured to evaluate the effect of AT-RvD1 treatment on cardiac inflammation. Histological analysis of cardiac tissue stained with hematoxylin-eosin was performed, and cellularity was quantified (Fig 4A). WT and FPR2$^{-/-}$ mice infected with *T. cruzi* (60 dpi) showed focal inflammatory infiltrates and increased cellularity in cardiac tissue. AT-RvD1 significantly reduced focal inflammatory infiltrates in the cardiac tissue (Fig 4B); the absence of FPR2 impaired the reduction in cellular infiltrates, suggesting that this receptor mediates the AT-

RvD1 effect. Moreover, the effect of AT-RvD1 in reducing the inflammatory infiltrates had a higher significance level than that obtained with Bz alone. Consistently, the combination of AT-Rv1 with Bz significantly reduced the inflammatory infiltrates in the WT mice, whereas, in the absence of FPR2, the reduction in inflammatory infiltrates achieved by combinatorial therapy was probably dependent on the effect of Bz.

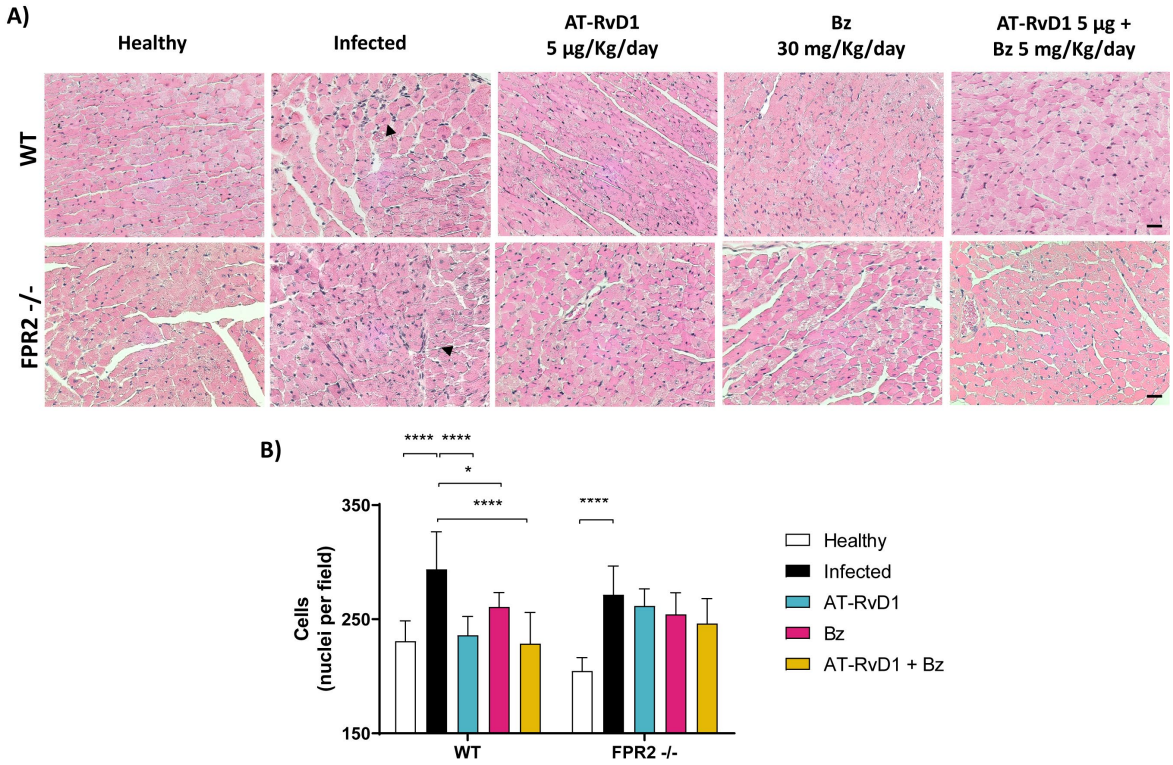

Fig 4. AT-RvD1 reduces cellular infiltrates in the heart tissue of C57BL/6 mice chronically infected with *Trypanosoma cruzi*. A) Representative images of heart tissue stained with hematoxylin and eosin from C57BL/6 mice infected with *T. cruzi* and treated with AT-RvD1 or benznidazole (Bz) at the indicated doses. Black arrows show infiltrated cells. Scale bar = 20 µm. B) Quantitative analysis of cellularity in cardiac tissues from five fields per animal. Data are expressed as the mean ± SD (n = 8). A two-way ANOVA and Tukey's post-hoc tests were performed to

344 identify significant differences. *p ≤ 0.05, ****p ≤ 0.0001. AT-RvD1, aspirin-triggered resolvin
345 D1.

346

347 Through FPR2, AT-RvD1 prevents cardiac remodeling in chronic CD

348 Because cardiac hypertrophy and dysfunction are significant complications of CCC, the effect of
349 AT-RvD1 on cardiac hypertrophy was assessed by measuring the cross-sectional area of
350 cardiomyocytes from heart tissue sections stained with hematoxylin-eosin (Fig 5A). *T. cruzi*
351 infection increased the cross-sectional area of cardiomyocytes in the WT and FPR2$^{-/-}$ mice after 60
352 dpi, demonstrating structural changes in the earliest phases of chronic disease. It is striking that in
353 healthy FPR2$^{-/-}$ mice, the cross-sectional areas were also increased compared with those in the WT
354 mice, which was consistent with the overall increase in circulating cytokine levels (Fig 2). Although
355 AT-RvD1 significantly reduced cardiomyocyte cross-sectional area, the effect was blunted by the
356 absence of FPR2 because in the FPR2$^{-/-}$ mice, there was no reduction in cardiac hypertrophy (Fig
357 5B). It is important to note that Bz alone did not affect cardiac hypertrophy; however, when
358 combined with AT-RvD1, it significantly reduced the cross-sectional area of cardiomyocytes in the
359 WT mice, but not in the absence of FPR2. These results suggest that AT-RvD1 therapy can reduce
360 cardiac hypertrophy. These observations were supported by measuring the mRNA levels of ANP
361 and BNP, molecular markers of cardiac hypertrophy (Fig 5C and D, respectively). Both ANP and
362 BNP were significantly increased in the infected WT and FPR2$^{-/-}$ mice (60 dpi), although the
363 changes in the FPR2$^{-/-}$ mice were negligible. Consistent with the histological analyses, treatment
364 with AT-RvD1 significantly reduced both molecular markers of cardiac hypertrophy. However, the
365 absence of FPR2 did not change the effect of AT-RvD1, suggesting that an alternative way
366 mediated this effect. Bz alone or combined with AT-RvD1 did not modify these molecular markers
367 of hypertrophy.

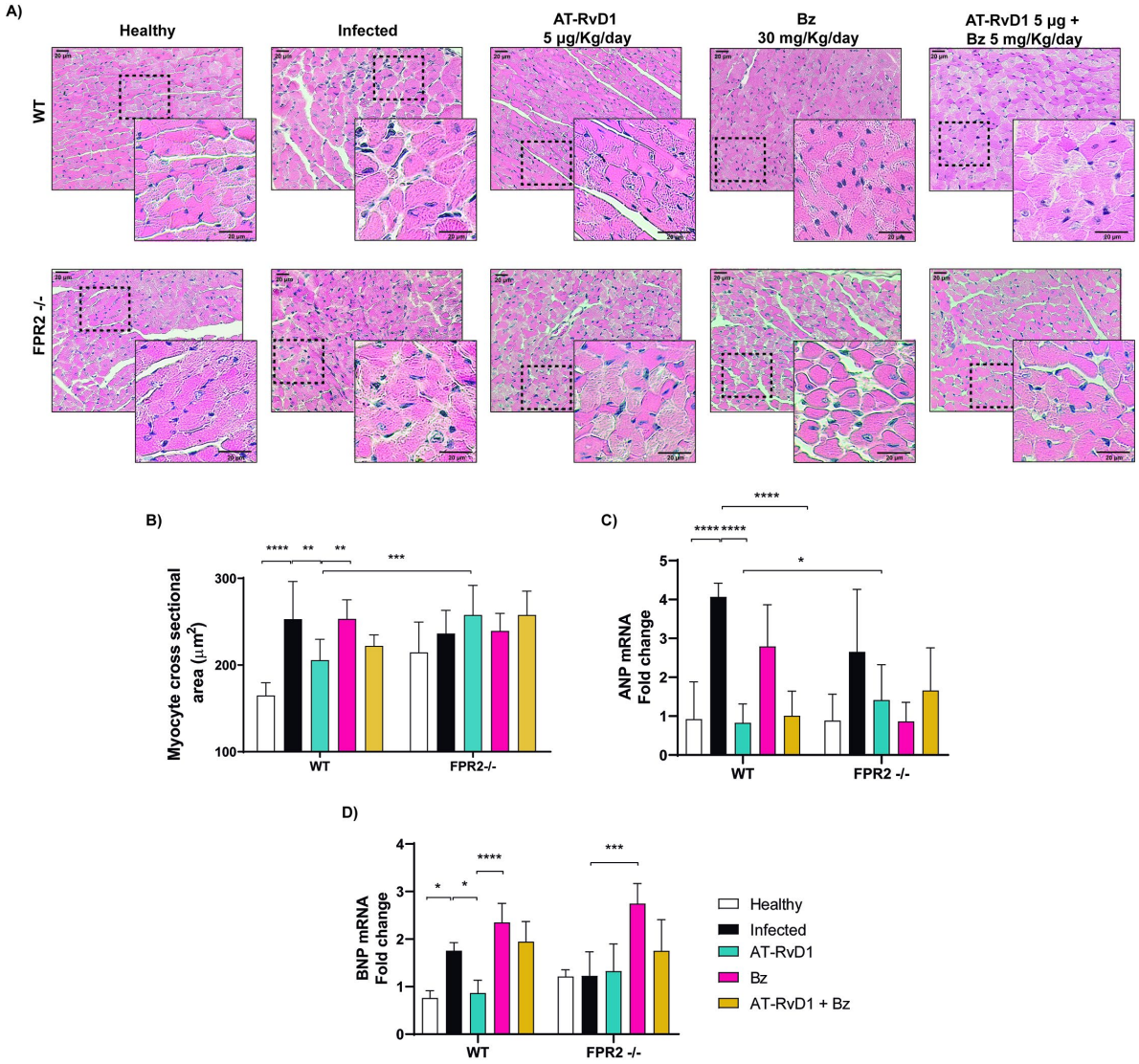

368

369 **Fig 5. AT-RvD1 reduces cardiac hypertrophy in C57BL/6 chronically infected with**
370 ***Trypanosoma cruzi.*** A) Images are enlargements of the representative images shown in Fig 4. B)
371 Analysis of the cross-sectional area of cardiomyocytes; 200 cardiomyocytes were randomly chosen
372 per animal. Scale bar = 20 µm. C, D) mRNA levels of atrial natriuretic peptide (ANP) and brain
373 natriuretic peptide (BNP), as markers of hypertrophy, are shown from cardiac tissue of C57BL/6
374 mice infected with *T. cruzi* and treated with AT-RvD1 and/or Bz, as measured by RT-qPCR. Data
375 are expressed as the mean ± SD (n = 5). Two-way ANOVAs and Tukey's post-hos tests were

performed to identify significant differences. *p ≤ 0.05, **p ≤ 0.01, ***p ≤ 0.001, ****p ≤ 0.0001. Bz, benznidazole; AT-RvD1, aspirin-triggered resolvin D1.

Although cardiac hypertrophy in chronic CD is a hallmark of cardiac remodeling, cardiac fibrosis reflects more profound structural damage. Thus, the effect of AT-RvD1 on cardiac fibrosis in CCC was analyzed in cardiac tissue stained with picrosirius red to visualize collagen fibers (Fig 6A). Consequently, cardiac fibrosis was increased with CD progression in both WT and FPR2$^{-/-}$ infected mice (60 dpi), and AT-RvD1 significantly reduced this cardiac fibrosis more efficiently than Bz in both genotypes.

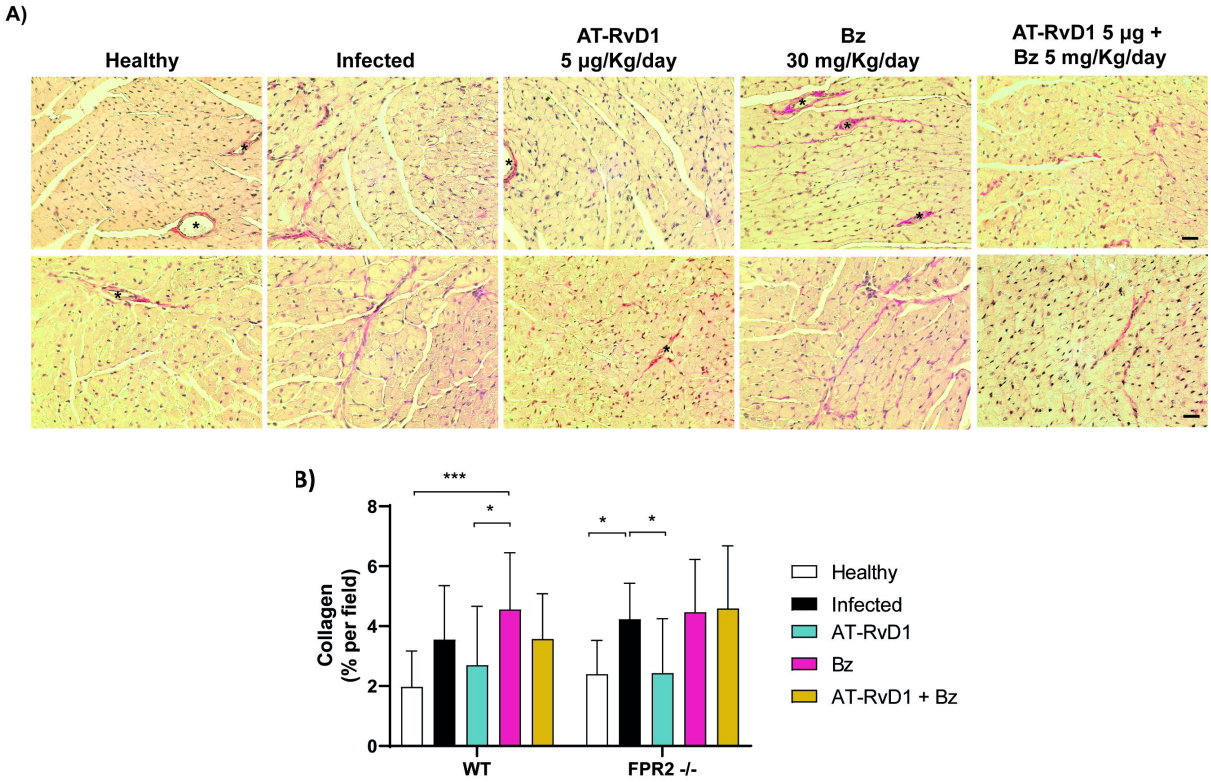

Fig 6. AT-RvD1 reduces cardiac fibrosis in C57BL/6 mice chronically infected with *Trypanosoma cruzi*. A) Representative images of picrosirius red-stained heart tissue from C57BL/6 mice infected with *T. cruzi* (Dm28c) and treated with AT-RvD1 or benznidazole (Bz) at the

389 indicated doses. Asterisks show blood vessels. Scale bar = 20 μm. B) Quantitative analysis of red
390 pixels in the stained cardiac tissue, corresponding to regions of fibrosis, from five fields per animal.
391 Data are expressed as the mean ± SD (n = 8). A two-way ANOVA and Tukey's post-hoc tests were
392 performed to identify significant differences. *$p \leq 0.05$, ***$p \leq 0.001$. AT-RvD1, aspirin-triggered
393 resolvin D1.

394 Signs of cardiac remodeling include atrioventricular and intraventricular conduction disorders such
395 as right bundle branch block, sinus bradycardia, and QT interval changes, alterations that may occur
396 early p.i. [21, 22]. Thus, the electrocardiographic activities of the C57BL/6 WT and FPR2$^{-/-}$ mice
397 were evaluated at the end of the treatments. However, at 60 dpi, no significant changes were found
398 in the ECG parameters of the mice (S2 Fig).

399 AT-RvD1 reduces parasite load in chronic CD

400 Cardiac parasite load was determined to verify establishment of the chronic phase and impact of the
401 treatments on parasite clearance. For this determination, RT-qPCR of *T. cruzi* 18S rRNA was
402 performed to determine parasite numbers in the cardiac tissue at the end of the treatments. As
403 expected, Bz reduced cardiac *T. cruzi* load to undetectable levels in both the WT and FPR2$^{-/-}$ mice
404 (Fig 7). However, a surprising finding was that AT-RvD1 decreased the cardiac *T. cruzi* load in the
405 WT and FPR2$^{-/-}$ mice, although the decrease in parasitic load was less marked in the null mice. This
406 finding was unexpected because AT-RvD1 does not have trypanocidal properties.

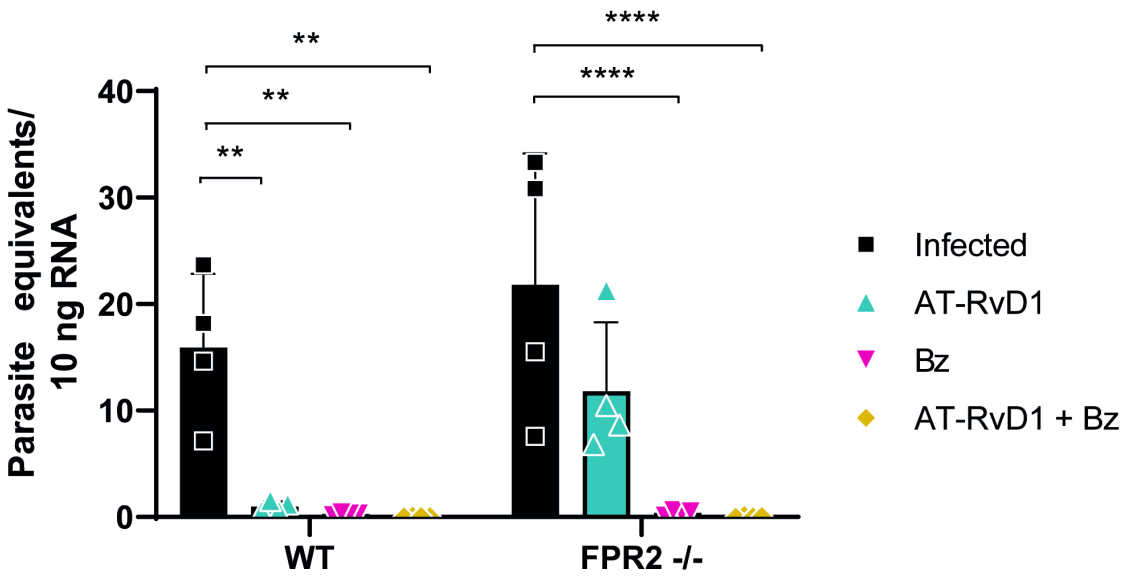

407

408 **Fig 7. Parasite load in cardiac tissue of mice chronically infected with *Trypanosoma cruzi* and**
409 **treated with AT-RvD1 and/or Bz at 60 dpi.** 18S rRNA from *T. cruzi* was detected by RT-qPCR.
410 Data are expressed as the mean ± SD (n = 4). Two-way ANOVA and Tukey's post-hoc tests were
411 performed to identify significant differences. **p ≤ 0.01, ****p ≤ 0.0001. Bz, benznidazole; AT-
412 RvD1, aspirin-triggered resolvin D1.

413

414 **Discussion**

415 Involvement of inflammation resolution in parasitemia control

416 In the experimental model used, the course of parasitemia in the WT mice was representative of the
417 behavior expected by the Dm28c strain of *T. cruzi* [14, 23]. In contrast, the FPR2$^{-/-}$ mice showed a
418 decrease in parasitemia. The latter results are consistent with other experimental models where the
419 deletion of 5-lipoxygenase (5-LO), which participates in the biosynthesis of lipoxins, also
420 developed reduced parasitemia [24, 25]. However, in other studies, 5-LO deficiency led to
421 increased parasitemia without affecting survival or infection control [26, 27]. These results suggest

422 that the breakdown of one or more pro-resolving elements of inflammation allows better control of
423 the parasite during the acute phase of the disease. This is probably caused by less containment of
424 the inflammatory response and an increased macrophage capability to eliminate parasites.
425 Specifically, parasitemia in the FPR2$^{-/-}$ mice was reduced after three weeks p.i., the time when an
426 adaptive antigen-specific response is established and cytotoxic and helper T lymphocytes and B
427 cells participate [28]. These responses could be more efficient in the FPR2$^{-/-}$ mice.

428 The WT and FPR2$^{-/-}$ mouse survival was similar and elevated throughout the experimental timeline,
429 probably because the C57BL/6 mouse lineage is resistant to infection with *T. cruzi* [29].
430 Interestingly, healthy FPR2$^{-/-}$ mice had elevated basal levels of IL-10 (S1 Fig), which could be
431 related to a lower risk of mortality during the acute phase of infection. In contrast, infected IL-10
432 knockout mice have a poor survival rate [30]. Thus, the anti-inflammatory balance mediated by IL-
433 10 likely plays a fundamental role in the survival and control of deleterious inflammatory
434 responses, probably mediated by Treg cell functions [25, 31].

435 The transition from acute to chronic phase is accompanied by decreased tissue parasitism and blood
436 parasitemia and control of the inflammatory response [32], which was observed in our experimental
437 model at 40 p.i.

438 <u>AT-RvD1 decreases the inflammatory process in chronic CD</u>

439 Our results showed that infection with *T. cruzi* triggers a robust inflammatory response in the acute
440 phase, with the production of inflammatory cytokines, such as IFNγ and TNFα, which have been
441 shown to activate macrophages to eliminate the parasite [32]. At day 60 p.i., the WT mice showed
442 slightly increased but sustained levels of the pro-inflammatory cytokines TNFα, IFNγ, and IL-1β,
443 reflecting an inflammatory state in the early stages of chronicity. Treatment with AT-RvD1 during
444 the early chronic phase significantly reduced the serum levels of IFNγ and IL-1β, producing an
445 immunoregulatory effect of the inflammatory state at the systemic level. These results are consistent

446 with previous studies, which have shown that PBMCs obtained from chagasic patients in stage B1
447 (the initial stage of CCC) treated with AT-RvD1 had lower IFNγ production than after antigenic re-
448 exposure to *T. cruzi*, and their cell proliferation was reduced, highlighting the immunomodulatory
449 effect of AT-RvD1 [18].

450 At the cardiac level, the scenario against *T. cruzi* is not very different. An imbalance is found, with
451 high levels of pro-inflammatory cytokines (TNFα, IFNγ, and IL-1β) and practically unchanged
452 levels of anti-inflammatory cytokines (IL-10). This could reflect the cell populations (including
453 macrophages, cytotoxic T lymphocytes, and helper T lymphocytes) infiltrating the cardiac tissue to
454 coordinate parasite control and represents an exacerbated production of cytokines related to tissue
455 destruction [6]. However, the participation of other cardiac cells such as fibroblasts, endothelial
456 cells, and cardiomyocytes has not been excluded [33]. Moreover, treatment with AT-RvD1
457 generates an immunomodulatory effect by drastically reducing the production of TNFα at the
458 cardiac level and suddenly increasing the production of IL-10. This suggests that AT-RvD1
459 increases the proportion of IL-10-producing cells (macrophage subpopulations, Treg and Breg cells)
460 in cardiac tissue to regulate the inflammatory environment.

461 Furthermore, the decrease in TNFα production may be secondary to the increase in IL-10 because
462 the latter is a potent inhibitor of TNFα mRNA expression through activation of the STAT3
463 transcription factor pathway in human monocytes and macrophages [34]. That would also explain
464 why, at the systemic level, we did not observe a reducing effect of TNFα. High levels of IL-10 have
465 been associated with evasion of the immune response by different pathogens, including *T. cruzi*
466 [35], contributing to increased mortality or persistence of damage [36]. However, high IL-10 levels
467 can also decrease inflammation and pathology; consequently, a pro/anti-inflammatory balance is
468 necessary for the natural evolution of the disease [37]. Nevertheless, elevated levels of IL-10 seem
469 to be related to maintaining adequate cardiac function in indeterminate patients with CD [38-40].
470 Therefore, the AT-RvD1 effect on IL-10 production in the heart appears to be beneficial for

471 preventing CCC progression since changes in IL-10 levels have been associated with losing the
472 ability to control the inflammatory immune response.

473 Although IFNγ is produced in the heart tissue by Th1 cell infiltrates in CCC, there was no change in
474 the mRNA of this cytokine after AT-RvD1 treatment. This finding does not correlate with the
475 corresponding IFNγ serum levels. However, AT-RvD1 reduced the inflammatory infiltrate in
476 cardiac tissue and was more efficient than Bz alone, probably mediated by reduced cellular and
477 vascular adhesion molecules (VCAM, ICAM) [41-43] in conjunction with modulation of the
478 inflammatory environment, as discussed above.

479 Previous studies have shown that the anti-inflammatory and pro-resolving properties of AT-RvD1
480 are primarily mediated by FPR2 [43]. In our model, FPR2 plays a fundamental role in regulating
481 pro-inflammatory and anti-inflammatory cytokines (IFNγ and IL-1B) and reducing cellular
482 infiltrates because its absence weakens the effect produced by AT-RvD1. Although the mechanism
483 of action of RvD1 is not fully understood, it has been shown to exert its anti-inflammatory effects
484 by inhibiting the NF-κB pathway [44, 45], suppressing cytosolic calcium, and decreasing activation
485 of the calcium-sensitive kinase calcium-calmodulin-dependent protein kinase II (CaMKII) [46].

486 Previous studies have shown that Bz, in addition to its trypanocidal properties, reduces cardiac cell
487 infiltrates and the production of inflammatory mediators via inhibition of the NF-κB pathway [5,
488 47-49], apparently, an effect dependent on IL-10 [50]. However, in the chronic CD model presented
489 herein, Bz did not regulate production of the pro-inflammatory (TNFα, IFNγ, and IL-1β) and anti-
490 inflammatory (IL-10) cytokines studied. Thus, there was only a slight reduction in the inflammatory
491 infiltrates with Bz treatment. Moreover, the combination of 5 mg/kg Bz and 5 μg/kg AT-RvD1
492 reduced cardiac inflammatory infiltrates but did not modulate the pro- and anti-inflammatory
493 cytokines studied. Unfortunately, no synergistic or additive effect could be observed between the
494 two drugs. Although both drugs act by inhibiting the NF-κB pathway, Bz could also increase

495 reactive oxygen species production at the tissue level [51, 52], contributing to the production and
496 establishment of a pro-inflammatory environment. This possibly explains why, although Bz is
497 effective as a trypanocidal therapy, it does not reduce the cardiovascular events observed in patients
498 with CCC [53].

499 The most recurrent lesion in advanced CCC is fibrosis and wall thinning, consistent with dilated
500 cardiomyopathy. Cardiomyocyte loss, due to parasite persistence and the consequent inflammatory
501 process, is characteristic of myocarditis, which is much less intense in indeterminate patients. Here,
502 cardiomyocyte hypertrophy was observed, evidenced by an increase in cell cross-sectional area and
503 correlated with elevated levels of natriuretic peptides, indicating hemodynamic overload. Together
504 with the interstitial fibrosis observed, these findings point to the presence of myocarditis
505 characteristic of CCC [7].

506 To the best of our knowledge, until now, the effect of AT-RvD1 on hypertrophy produced by
507 infection with *T. cruzi* had not been studied. Herein, AT-RvD1 was shown to reduce both the cross-
508 sectional area of cardiomyocytes and the transcription of hypertrophy markers such as ANP and
509 BNP, which have been associated with different stages and severity of CCC [54, 55]. Furthermore,
510 during *T. cruzi* infection, the participation of endothelin-1, cardiotrophin-1, and cytokines such as
511 TNFα and IL-1β has been previously highlighted as pro-hypertrophic [56]. Therefore, the effect of
512 AT-RvD1 on hypertrophy could also be a consequence of its immunoregulatory effect [57].
513 Although FPR2 mediates the anti-hypertrophic effect of AT-RvD1, it also activates G protein-
514 coupled receptor 23 (GPR23) [58]. Thus, GPR32 participation may be an alternative pathway for
515 the action of AT-RvD1, explaining the changes in ANP and BNP expression observed in the $FPR2^{-/-}$
516 mice.

517 Additionally, AT-RvD1 reduced cardiac fibrosis in our experimental model. This finding is
518 consistent with that of a previous report showing that the administration of RvD1 to mice infected

519 with *T. cruzi* reduced cardiac fibrosis and transforming growth factor-β (TGF-β) mRNA levels in
520 the heart [19]. However, we used a 20-day continuous treatment scheme during the chronic stage of
521 infection instead of the three-bolus scheme used by the previous investigators. In experimental
522 models of myocardial infarction, RvD1 reduced the transcription of profibrotic genes and decreased
523 collagen deposition, thereby reducing fibrosis and improving ventricular function [59]. The effect of
524 AT-RvD1 on fibrosis is not dependent on FPR2 exclusively since the antifibrotic effect exerted by
525 AT-RvD1 was not impaired in the $FPR2^{-/-}$ mice. Therefore, we propose that GPR32 may be
526 necessary for this purpose, suggesting a level of redundancy within the resolution of the
527 inflammation cascade.

528 An electrocardiographic analysis performed on the infected animals showed alterations in the QT
529 interval in the WT mice, suggesting a slowdown in ventricular repolarization. This alteration
530 appears early in patients with CCC and is a mortality predictor in patients with CD [60, 61].
531 Although this QT interval alteration helped confirm the model's chronic nature, AT-RvD1 did not
532 affect this disease pathology. A more prolonged observation period may be necessary to observe
533 significant AT-RvD1-dependent changes in electrical cardiac function.

534 AT-RvD1 reduces parasite load in *T. cruzi*-infected mice

535 Importantly, AT-RvD1 has no trypanocidal activity. However, we observed that AT-RvD1 alone or
536 combined with Bz reduced the heart parasite load in infected mice. Studies in experimental CCC
537 models have indicated that the administration of 15-epi-LXA_4 similarly reduces the parasite load of
538 cardiac tissue in infected mice [24]. In the absence of FPR2, eliminating the parasite from cardiac
539 tissue is not as efficient, suggesting that the pro-resolving cascade is essential for promoting
540 parasite clearance. Probably, the anti-inflammatory effect of AT-RvD1 reduces the deleterious
541 effect of the inflammatory environment that favors parasite persistence. The pro-resolving processes

542 initiated by AT-RvD1 enable the immune system to eliminate the parasites, probably because
543 chronic inflammation is an evasive mechanism used by the parasites.

544 In conclusion, current drug therapies are ineffective in all phases of CD and they do not prevent
545 long-term loss of heart function. Thus, the resolution of inflammation is advantageous as a
546 pharmacological strategy for CCC. FPR2-dependent AT-RvD1 is a pro-resolving lipid mediator
547 effective against inflammation, dampening pathological inflammatory responses and restoring
548 tissue homeostasis; importantly, it contributes to clearing adverse inflammatory environments and
549 allowing more efficient parasite elimination. Consequently, drug strategies aimed to modify host
550 factors and resolve inflammation will improve specific antiparasitic drug therapy in the future.

551 **Acknowledgments**

552 The authors wish to acknowledge grant funding from Agencia Nacional de Investigación y
553 Desarrollo (ANID) FONDECYT grants 1210359 (JDM), 1190341 (UK), 1210627 (GD), 3210667
554 (SF) and 3180452 (CC); BECAS ANID grant 21170501 (IC), 21170427 (FG) and 21170968 (HQ);
555 Conselho Nacional de Desenvolvimento Científico e Tecnológico (CNPq: 305894/2018-8), and
556 Fundação de Amparo a Pesquisa de Minas Gerais (Rede Mineira de Imunobiológicos, REDE-
557 00140-16) (FSM). In addition, the authors wish to thank Dr. Jader Dos Santos Cruz from the
558 Department of Biochemistry and Immunology, Institute of Biological Sciences, Federal University
559 of Minas Gerais, Brazil, for performing the mouse electrocardiograms.

560

561 **References:**

562 1. WHO. Chagas disease (also known as American trypanosomiasis). Fact Sheets: WHO
563 2020: WHO 2020 [cited 2021 August 10]. Available from: https://www.who.int/news-
564 room/fact-sheets/detail/chagas-disease-(american-trypanosomiasis).

565 2. Coura JR. Chagas disease: what is known and what is needed--a background article. Mem
566 Inst Oswaldo Cruz. 2007;102 Suppl 1:113-22.
567 3. Perez-Molina JA, Molina I. Chagas disease. Lancet. 2018;391(10115):82-94.
568 4. Echeverria LE, Morillo CA. American Trypanosomiasis (Chagas Disease). Infect Dis Clin
569 North Am. 2019;33(1):119-34.
570 5. Rassi A, Jr., Marin JAN, Rassi A. Chronic Chagas cardiomyopathy: a review of the main
571 pathogenic mechanisms and the efficacy of aetiological treatment following the
572 BENznidazole Evaluation for Interrupting Trypanosomiasis (BENEFIT) trial. Mem Inst
573 Oswaldo Cruz. 2017:0.
574 6. Acevedo GR, Girard MC, Gomez KA. The Unsolved Jigsaw Puzzle of the Immune
575 Response in Chagas Disease. Front Immunol. 2018;9:1929.
576 7. Bonney KM, Luthringer DJ, Kim SA, Garg NJ, Engman DM. Pathology and Pathogenesis
577 of Chagas Heart Disease. Annu Rev Pathol. 2019;14:421-47.
578 8. Serhan CN. Discovery of specialized pro-resolving mediators marks the dawn of resolution
579 physiology and pharmacology. Mol Aspects Med. 2017;58:1-11.
580 9. Serhan CN, Arita M, Hong S, Gotlinger K. Resolvins, docosatrienes, and neuroprotectins,
581 novel omega-3-derived mediators, and their endogenous aspirin-triggered epimers. Lipids.
582 2004;39(11):1125-32.
583 10. Serhan CN, Levy BD. Resolvins in inflammation: emergence of the pro-resolving
584 superfamily of mediators. J Clin Invest. 2018;128(7):2657-69.
585 11. Sun YP, Oh SF, Uddin J, Yang R, Gotlinger K, Campbell E, et al. Resolvin D1 and its
586 aspirin-triggered 17R epimer. Stereochemical assignments, anti-inflammatory properties,
587 and enzymatic inactivation. J Biol Chem. 2007;282(13):9323-34.
588 12. Serhan CN. Pro-resolving lipid mediators are leads for resolution physiology. Nature.
589 2014;510(7503):92-101.

590 13. Lopez-Munoz RA, Molina-Berrios A, Campos-Estrada C, Abarca-Sanhueza P, Urrutia-
591 Llancaqueo L, Pena-Espinoza M, et al. Inflammatory and Pro-resolving Lipids in
592 Trypanosomatid Infections: A Key to Understanding Parasite Control. Front Microbiol.
593 2018;9:1961.
594 14. Molina-Berrios A, Campos-Estrada C, Lapier M, Duaso J, Kemmerling U, Galanti N, et al.
595 Protection of vascular endothelium by aspirin in a murine model of chronic Chagas' disease.
596 Parasitol Res. 2013;112(7):2731-9.
597 15. Carvalho de Freitas R, Lonien SCH, Malvezi AD, Silveira GF, Wowk PF, da Silva RV, et
598 al. Trypanosoma cruzi: Inhibition of infection of human monocytes by aspirin. Exp
599 Parasitol. 2017;182:26-33.
600 16. Malvezi AD, Panis C, da Silva RV, de Freitas RC, Lovo-Martins MI, Tatakihara VL, et al.
601 Inhibition of cyclooxygenase-1 and cyclooxygenase-2 impairs Trypanosoma cruzi entry
602 into cardiac cells and promotes differential modulation of the inflammatory response.
603 Antimicrob Agents Chemother. 2014;58(10):6157-64.
604 17. Carlo T, Kalwa H, Levy BD. 15-Epi-lipoxin A4 inhibits human neutrophil superoxide
605 anion generation by regulating polyisoprenyl diphosphate phosphatase 1. FASEB J.
606 2013;27(7):2733-41. doi: 10.1096/fj.12-223982.
607 18. Ogata H, Teixeira MM, Sousa RC, Silva MV, Correia D, Rodrigues Junior V, et al. Effects
608 of aspirin-triggered resolvin D1 on peripheral blood mononuclear cells from patients with
609 Chagas' heart disease. Eur J Pharmacol. 2016;777:26-32.
610 19. Horta AL, Williams T, Han B, Ma Y, Menezes APJ, Tu V, et al. Resolvin D1
611 Administration Is Beneficial in Trypanosoma cruzi Infection. Infect Immun. 2020;88(6).
612 doi: 10.1128/IAI.00052-20.
613 20. Pfaffl MW. A new mathematical model for relative quantification in real-time RT-PCR.
614 Nucleic Acids Res. 2001;29(9):e45.

615 21. Soverow J, Hernandez S, Sanchez D, Forsyth C, Flores CA, Viana G, et al. Progression of
616 Baseline Electrocardiogram Abnormalities in Chagas Patients Undergoing
617 Antitrypanosomal Treatment. Open Forum Infect Dis. 2019;6(2):ofz012.
618 22. Marcolino MS, Palhares DM, Ferreira LR, Ribeiro AL. Electrocardiogram and Chagas
619 disease: a large population database of primary care patients. Glob Heart. 2015;10(3):167-
620 72.
621 23. Molina-Berrios A, Campos-Estrada C, Henriquez N, Faundez M, Torres G, Castillo C, et al.
622 Protective role of acetylsalicylic acid in experimental Trypanosoma cruzi infection:
623 evidence of a 15-epi-lipoxin A(4)-mediated effect. PLoS Negl Trop Dis. 2013;7(4):e2173.
624 24. Gonzalez-Herrera F, Cramer A, Pimentel P, Castillo C, Liempi A, Kemmerling U, et al.
625 Simvastatin Attenuates Endothelial Activation through 15-Epi-Lipoxin A4 Production in
626 Murine Chronic Chagas Cardiomyopathy. Antimicrob Agents Chemother. 2017;61(3).
627 25. Esper L, Roman-Campos D, Lara A, Brant F, Castro LL, Barroso A, et al. Role of SOCS2
628 in modulating heart damage and function in a murine model of acute Chagas disease. Am J
629 Pathol. 2012;181(1):130-40.
630 26. Canavaci AM, Sorgi CA, Martins VP, Morais FR, de Sousa EV, Trindade BC, et al. The
631 acute phase of Trypanosoma cruzi infection is attenuated in 5-lipoxygenase-deficient mice.
632 Mediators Inflamm. 2014;2014:893634.
633 27. Pavanelli WR, Gutierrez FR, Mariano FS, Prado CM, Ferreira BR, Teixeira MM, et al. 5-
634 lipoxygenase is a key determinant of acute myocardial inflammation and mortality during
635 Trypanosoma cruzi infection. Microbes Infect. 2010;12(8-9):587-97.
636 28. Cardillo F, de Pinho RT, Antas PR, Mengel J. Immunity and immune modulation in
637 Trypanosoma cruzi infection. Pathog Dis. 2015;73(9):ftv082.
638 29. Ferreira BL, Ferreira ER, de Brito MV, Salu BR, Oliva MLV, Mortara RA, et al. BALB/c
639 and C57BL/6 Mice Cytokine Responses to Trypanosoma cruzi Infection Are Independent
640 of Parasite Strain Infectivity. Front Microbiol. 2018;9:553.

641 30. Roffe E, Rothfuchs AG, Santiago HC, Marino AP, Ribeiro-Gomes FL, Eckhaus M, et al.
642 IL-10 limits parasite burden and protects against fatal myocarditis in a mouse model of
643 Trypanosoma cruzi infection. J Immunol. 2012;188(2):649-60.
644 31. Tonelli RR, Torrecilhas AC, Jacysyn JF, Juliano MA, Colli W, Alves MJ. In vivo infection
645 by Trypanosoma cruzi: the conserved FLY domain of the gp85/trans-sialidase family
646 potentiates host infection. Parasitology. 2011;138(4):481-92.
647 32. Dutra WO, Menezes CA, Magalhaes LM, Gollob KJ. Immunoregulatory networks in
648 human Chagas disease. Parasite Immunol. 2014;36(8):377-87.
649 33. Machado FS, Martins GA, Aliberti JC, Mestriner FL, Cunha FQ, Silva JS. Trypanosoma
650 cruzi-infected cardiomyocytes produce chemokines and cytokines that trigger potent nitric
651 oxide-dependent trypanocidal activity. Circulation. 2000;102(24):3003-8.
652 34. Chan CS, Ming-Lum A, Golds GB, Lee SJ, Anderson RJ, Mui AL. Interleukin-10 inhibits
653 lipopolysaccharide-induced tumor necrosis factor-alpha translation through a SHIP1-
654 dependent pathway. J Biol Chem. 2012;287(45):38020-7.
655 35. Reed SG, Brownell CE, Russo DM, Silva JS, Grabstein KH, Morrissey PJ. IL-10 mediates
656 susceptibility to Trypanosoma cruzi infection. J Immunol. 1994;153(7):3135-40.
657 36. Anderson CF, Mendez S, Sacks DL. Nonhealing infection despite Th1 polarization
658 produced by a strain of Leishmania major in C57BL/6 mice. J Immunol. 2005;174(5):2934-
659 41.
660 37. Iyer SS, Cheng G. Role of interleukin 10 transcriptional regulation in inflammation and
661 autoimmune disease. Crit Rev Immunol. 2012;32(1):23-63.
662 38. Vasconcelos RH, Azevedo Ede A, Diniz GT, Cavalcanti Mda G, de Oliveira W, Jr., de
663 Morais CN, et al. Interleukin-10 and tumour necrosis factor-alpha serum levels in chronic
664 Chagas disease patients. Parasite Immunol. 2015;37(7):376-9.

665 39. Sousa GR, Gomes JA, Fares RC, Damasio MP, Chaves AT, Ferreira KS, et al. Plasma
666 cytokine expression is associated with cardiac morbidity in chagas disease. PLoS One.
667 2014;9(3):e87082.
668 40. Gomes JA, Bahia-Oliveira LM, Rocha MO, Busek SC, Teixeira MM, Silva JS, et al. Type 1
669 chemokine receptor expression in Chagas' disease correlates with morbidity in cardiac
670 patients. Infect Immun. 2005;73(12):7960-6.
671 41. Salas-Hernandez A, Espinoza-Perez C, Vivar R, Espitia-Corredor J, Lillo J, Parra-Flores P,
672 et al. Resolvin D1 and E1 promote resolution of inflammation in rat cardiac fibroblast in
673 vitro. Mol Biol Rep. 2021;48(1):57-66.
674 42. Chen J, Shetty S, Zhang P, Gao R, Hu Y, Wang S, et al. Aspirin-triggered resolvin D1
675 down-regulates inflammatory responses and protects against endotoxin-induced acute
676 kidney injury. Toxicol Appl Pharmacol. 2014;277(2):118-23.
677 43. Bento AF, Claudino RF, Dutra RC, Marcon R, Calixto JB. Omega-3 fatty acid-derived
678 mediators 17(R)-hydroxy docosahexaenoic acid, aspirin-triggered resolvin D1 and resolvin
679 D2 prevent experimental colitis in mice. J Immunol. 2011;187(4):1957-69.
680 44. Lee HN, Kundu JK, Cha YN, Surh YJ. Resolvin D1 stimulates efferocytosis through
681 p50/p50-mediated suppression of tumor necrosis factor-alpha expression. J Cell Sci.
682 2013;126(Pt 17):4037-47.
683 45. Gao Y, Zhang H, Luo L, Lin J, Li D, Zheng S, et al. Resolvin D1 Improves the Resolution
684 of Inflammation via Activating NF-kappaB p50/p50-Mediated Cyclooxygenase-2
685 Expression in Acute Respiratory Distress Syndrome. J Immunol. 2017.
686 46. Fredman G, Ozcan L, Spolitu S, Hellmann J, Spite M, Backs J, et al. Resolvin D1 limits 5-
687 lipoxygenase nuclear localization and leukotriene B4 synthesis by inhibiting a calcium-
688 activated kinase pathway. Proc Natl Acad Sci U S A. 2014;111(40):14530-5.
689 47. Piaggio E, Sanceau J, Revelli S, Bottasso O, Wietzerbin J, Serra E. Trypanocidal drug
690 benznidazole impairs lipopolysaccharide induction of macrophage nitric oxide synthase

691 gene transcription through inhibition of NF-kappaB activation. J Immunol.
692 2001;167(6):3422-6.
693 48. Cevey AC, Mirkin GA, Penas FN, Goren NB. Low-dose benznidazole treatment results in
694 parasite clearance and attenuates heart inflammatory reaction in an experimental model of
695 infection with a highly virulent Trypanosoma cruzi strain. Int J Parasitol Drugs Drug Resist.
696 2016;6(1):12-22.
697 49. Garcia S, Ramos CO, Senra JF, Vilas-Boas F, Rodrigues MM, Campos-de-Carvalho AC, et
698 al. Treatment with benznidazole during the chronic phase of experimental Chagas' disease
699 decreases cardiac alterations. Antimicrob Agents Chemother. 2005;49(4):1521-8.
700 50. Cevey AC, Penas FN, Alba Soto CD, Mirkin GA, Goren NB. IL-10/STAT3/SOCS3 Axis Is
701 Involved in the Anti-inflammatory Effect of Benznidazole. Front Immunol. 2019;10:1267.
702 doi: 10.3389/fimmu.2019.01267.
703 51. Ribeiro CM, Budni P, Pedrosa RC, Farias MS, Parisotto EB, Dalmarco EM, et al.
704 Antioxidant therapy attenuates oxidative insult caused by benzonidazole in chronic Chagas'
705 heart disease. Int J Cardiol. 2010;145(1):27-33.
706 52. Hall BS, Wilkinson SR. Activation of benznidazole by trypanosomal type I nitroreductases
707 results in glyoxal formation. Antimicrob Agents Chemother. 2012;56(1):115-23.
708 53. Morillo CA, Marin-Neto JA, Avezum A, Sosa-Estani S, Rassi A, Jr., Rosas F, et al.
709 Randomized Trial of Benznidazole for Chronic Chagas' Cardiomyopathy. N Engl J Med.
710 2015;373(14):1295-306.
711 54. Echeverria LE, Rojas LZ, Calvo LS, Roa ZM, Rueda-Ochoa OL, Morillo CA, et al. Profiles
712 of cardiovascular biomarkers according to severity stages of Chagas cardiomyopathy. Int J
713 Cardiol. 2017;227:577-82.
714 55. Tucci AR, Oliveira FOR, Jr., Lechuga GC, Oliveira GM, Eleuterio AC, Mesquita LB, et al.
715 Role of FAK signaling in chagasic cardiac hypertrophy. Braz J Infect Dis. 2020;24(5):386-
716 97.

717 56. Corral RS, Guerrero NA, Cuervo H, Girones N, Fresno M. Trypanosoma cruzi infection
718 and endothelin-1 cooperatively activate pathogenic inflammatory pathways in
719 cardiomyocytes. PLoS Negl Trop Dis. 2013;7(2):e2034.
720 57. Petersen CA, Burleigh BA. Role for interleukin-1 beta in Trypanosoma cruzi-induced
721 cardiomyocyte hypertrophy. Infect Immun. 2003;71(8):4441-7.
722 58. Pirault J, Back M. Lipoxin and Resolvin Receptors Transducing the Resolution of
723 Inflammation in Cardiovascular Disease. Front Pharmacol. 2018;9:1273.
724 59. Kain V, Ingle KA, Colas RA, Dalli J, Prabhu SD, Serhan CN, et al. Resolvin D1 activates
725 the inflammation resolving response at splenic and ventricular site following myocardial
726 infarction leading to improved ventricular function. J Mol Cell Cardiol. 2015;84:24-35.
727 60. Salles G, Xavier S, Sousa A, Hasslocher-Moreno A, Cardoso C. Prognostic value of QT
728 interval parameters for mortality risk stratification in Chagas' disease: results of a long-term
729 follow-up study. Circulation. 2003;108(3):305-12.
730 61. Eickhoff CS, Lawrence CT, Sagartz JE, Bryant LA, Labovitz AJ, Gala SS, et al. ECG
731 detection of murine chagasic cardiomyopathy. J Parasitol. 2010;96(4):758-64.
732
733
734